



Agbani, E. O., Zhao, X., Williams, C. M., Aungraheeta, R., Hers, I., Swenson, E. R., & Poole, A. W. (2020). Carbonic Anhydrase Inhibitors Suppress Platelet Procoagulant Responses and In Vivo Thrombosis. *Platelets*. <https://doi.org/10.1080/09537104.2019.1709632>

Peer reviewed version

License (if available):
Unspecified

Link to published version (if available):
[10.1080/09537104.2019.1709632](https://doi.org/10.1080/09537104.2019.1709632)

[Link to publication record in Explore Bristol Research](#)
PDF-document

This is the author accepted manuscript (AAM). The final published version (version of record) is available online via Taylor & Francis at <https://www.tandfonline.com/doi/full/10.1080/09537104.2019.1709632> . Please refer to any applicable terms of use of the publisher.

University of Bristol - Explore Bristol Research

General rights

This document is made available in accordance with publisher policies. Please cite only the published version using the reference above. Full terms of use are available: <http://www.bristol.ac.uk/red/research-policy/pure/user-guides/ebr-terms/>

Carbonic Anhydrase Inhibitors Suppress Platelet Procoagulant Responses and In Vivo Thrombosis

Ejaife O. Agbani^{1, 2, 3, #} BPharm, MSc, PhD; Xiaojuan Zhao¹ MA PhD; Christopher M. Williams¹ BSc, PhD; Riyaad Aungraheeta¹ BSc, MSc, PhD; Ingeborg Hers¹ BSc, MSc, PhD; Erik R. Swenson⁴ MD; Alastair W. Poole¹ # MA, PhD, VetMB

1. School of Physiology, Pharmacology and Neuroscience, University of Bristol, Medical Sciences Building, Bristol, BS8 1TD, United Kingdom.
2. Department of Physiology and Pharmacology, Cumming School of Medicine, University of Calgary, Alberta, Canada
3. Libin Cardiovascular Institute of Alberta, Vascular Basic Science, Calgary, Alberta, Canada
4. Division of Pulmonary, Critical Care and Sleep Medicine, Medical Service, VA Puget Sound Health Care System, University of Washington, Seattle WA, USA

#: Address correspondence to :

Ejaife O. Agbani [BPharm, MSc, PhD; Email: ejaiife.agbani@ucalgary.ca]
Libin Cardiovascular Institute of Alberta, 3330 Hospital Drive NW
Calgary, T2N 4N1 Alberta, Canada

Short Title: Carbonic Anhydrase Inhibitors as Antithrombotics

ABSTRACT

Carbonic anhydrase (CA) inhibitors have a long history of safe clinical use as mild diuretics, in the treatment of glaucoma and for altitude sickness prevention. In this study, we aimed to determine if CA inhibition may be an alternative approach to control thrombosis. We utilised a high-resolution dynamic imaging approach to provide mechanistic evidence that CA inhibitors may be potent anti-procoagulant agents *in vitro* and effective anti-thrombotics *in vivo*. Acetazolamide and methazolamide, while sparing platelet secretion, attenuated intracellular chloride ion entry and suppressed the procoagulant response of activated platelets *in vitro* and thrombosis *in vivo*. The chemically similar N-methyl acetazolamide, which lacks CA inhibitory activity, did not affect platelet procoagulant response *in vitro*. Outputs from rotational thromboelastometry did not reflect changes in procoagulant activity and reveal the need for a suitable clinical test for procoagulant activity. Drugs specifically targeting procoagulant remodelling of activated platelets, by blockade of carbonic anhydrases, may provide a new way to control platelet-driven thrombosis without blocking essential platelet secretion responses.

KEYWORDS

Platelets Procoagulant Membrane Dynamics, Carbonic Anhydrase, Methazolamide, Acetazolamide

INTRODUCTION

Collagen stimulation of platelets has been shown to increase the formation of a procoagulant phenotype amongst platelets aggregating over exposed sub-endothelium [1, 2]. Procoagulant platelets actively support thrombin generation and amplify coagulation by providing an extensive surface area of exposed aminophospholipids, particularly phosphatidylserine (PS), which promotes assembly of the tenase and prothrombinase complexes on the platelet surface [3, 4]. This subpopulation of platelets is characterised by PS-laden balloon-like membranes and by microvesiculation, amongst other features [4-7]. Recently, we identified two phenotypes of this subpopulation as ballooned non-spread (BNS) and ballooned and procoagulant-spread platelets (BAPS) [4, 6-8]. Furthermore, we showed that selective inhibition of their formation either by pharmacological inhibition or by water channel aquaporin-1 gene ablation did not impair secretion mechanisms, yet suppressed procoagulation *in vitro* and thrombus formation *in vivo* after injury [6]. Therefore, drugs specifically targeting procoagulant platelet formation may provide a new way to control platelet driven thrombosis without blocking essential platelet granular releasates.

The potent carbonic anhydrase enzyme (CA) inhibitors acetazolamide (ACZ) and methazolamide (MTZ) have been used extensively clinically as weak diuretic agents, in the treatment of glaucoma and prevention of altitude sickness [9]. Previously, we showed that CA inhibitor ACZ inhibited thrombosis *in vivo* and procoagulant activity *in vitro*; in this report, we provide further mechanistic evidence that extends this finding and shows that the CA inhibitor MTZ is also a potent anti-procoagulant *in vitro* and effective antithrombotic *in vivo*. Importantly, these inhibitors have the potential to be a genuinely novel approach to the management of thrombotic diseases, since we have recently shown that blockade of P2Y₁ and P2Y₁₂ receptors, which underlies the actions of several antithrombotics in clinical use, particularly P2Y₁₂, does not inhibit platelet procoagulant membrane ballooning or microvesiculation [5].

MATERIAL AND METHODS

Materials: Fibrillar collagen (Horm suspension) was from Nycomed (Munich, Germany). Alexa Fluor® 568 conjugated annexin V (annexin-V; anxV) and Fluo-4 AM, were purchased from Life Technologies. Glass bottom 35mm dishes (P35G-1.5-14-C) were obtained from MatTek Corporation (USA). Antibodies to carbonic anhydrase CA I (Cat # sc-50899; [sc-393528](#)), and CA II (Cat # sc-48351) were from Santa Cruz; Anti-CA XIII antibody was from Abcam (Cat # ab135986)

Human Platelet Rich Plasma and Washed Platelet Preparation: Human blood was obtained from healthy drug-free volunteers, who gave full informed consent in accordance with the Declaration of Helsinki, with approval from the local research ethics committee of the University of Bristol. Blood drawn was anticoagulated with 0.4% trisodium citrate and centrifuged at 180 g for 17 min, to prepare platelet-rich plasma (PRP). To obtain washed platelets, PRP was centrifuged at 650 g for 10 minutes in the presence of 10 µM indomethacin and 0.02 U/mL apyrase. Pelleted platelets were re-suspended in Tyrode's-HEPES buffer, counted using a Z1 Coulter particle counter (Beckman Coulter, High Wycombe, UK), diluted to the required concentration in modified HEPES-Tyrode buffer modified with 0.1% (wt/vol) glucose and rested for least 30 min at 30°C before experimentation.

Mouse Washed Platelet Preparation: Mice were bred and maintained in the University of Bristol animal facility in accordance with United Kingdom Home Office regulations. All procedures were undertaken with United Kingdom Home Office approval in accordance with the Animals (Scientific Procedures) Act of 1986 (PPL30/3445). Blood was drawn into 4% trisodium citrate (1:9) by descending vena cava puncture of mice humanely killed by rising CO₂ inhalation [Animals Act Schedule 1 (1986)]. Prior to platelet preparation, full blood counts were conducted using a Pentra ES60 hematology analyser (Horiba Medical, Northampton, UK) and values adjusted for anticoagulant volume. Washed platelets were prepared by diluting withdrawn blood with 800 µl of modified Tyrode's-HEPES buffer (135 mM NaCl, 3 mM KCl, 10 mM HEPES, 5 mM glucose, and 1 mM MgCl₂·6 H₂O, pH 7.3) and centrifuged at 180 g for 6 min at room temperature. Platelet-rich plasma was removed, and platelets were isolated by centrifugation at 550 g for 10 min in the presence of indomethacin (10 µM) and apyrase (0.02 U/ml). Pelleted platelets were re-suspended in Tyrode's-HEPES buffer, counted using a Z1 Coulter particle counter (Beckman Coulter, High Wycombe, UK), diluted to the required concentration in modified Tyrode's-HEPES buffer and rested for least 30 min at 30°C before experimentation.

Turbidometric Aggregometry and ATP Secretion: Agonist induced platelet aggregation was assessed utilizing a Born lumi-aggregometer (560-VS, Chrono-Log) in aliquots of washed platelets (245 µl of 2x10⁸/ml) or platelet-rich plasma stirred at 1000 rpm (37 °C). Simultaneously, ATP secretion was measured using a luciferin-luciferase assay calibrated with 2 nmol of ATP standards.

Flow cytometry: Two-color analysis of the kinetics of platelet activation was conducted with the FITC-conjugated PAC-1 antibody to assess integrin αIIbβ₃ activation and PE-conjugated anti-P-selectin (CD62P) to assess α-granule secretion. Aliquots of platelets (2 × 10⁷ mL⁻¹) in modified HEPES-Tyrode buffer containing 10 µM indomethacin, 0.02 U/ml apyrase, 0.1% [w/v] D-glucose, and 1 mM CaCl₂ were

treated with vehicle (0.2% DMSO) or Car inhibitors ($100 \mu\text{mol L}^{-1}$) for 15 min before stimulation with agonists at time 'zero.' Agonist stimulation (10 minutes) was in the presence of FITC-PAC-1 and PE-anti-P-selectin before fixation with 1% paraformaldehyde for 30 minutes. Two-color fluorescent analysis was conducted on a FACSCalibur flow cytometer (BD Biosciences) using FACSDiva software. Based on forward and side scatter, the platelet population was gated and 20,000 events were captured.

Immunoblotting: Washed platelets ($4 \times 10^8/\text{ml}$) stimulated as indicated, were lysed in Laemmli buffer containing 50 mM dithiothreitol. Proteins were separated by electrophoresis using 8–15% Tris glycine-polyacrylamide gels against known molecular weight markers and transferred onto PVDF membranes. After blocking with 5% BSA in Tris-buffered saline/Tween-20 (10 mM Tris, 150 mM NaCl, and 0.1% Tween 20), membranes were probed with the appropriate primary and horseradish peroxidase-conjugated secondary antibodies, and proteins were detected by enhanced chemiluminescence.

Confocal Microscopy: Confocal images were acquired using a Perkin Elmer Ultra-VIEW ERS 6FE confocal system (with Yokogawa CSU22 spinning disk) attached to a Leica DM I6000 inverted epifluorescence microscope. The system is equipped with Piezo drive, Hamamatsu C9100-50 EM-CCD camera (14 bit, 8 micron pixels) and the following laser lines: 14 mW Ar laser (488, 514 nm lines), 7.5 mW Kr laser (568 nm), 7.5 mW violet (405 nm) diode laser, 7mW blue diode laser (440 nm) and 7.5 mW Red diode (640 nm). Images were captured with Volocity (PerkinElmer) acquisition software using an oil immersion objective lens (100x). Acquisition setting was kept constant, and pixel width at x1 binning was $0.069 \mu\text{m}$; phase-contrast imaging was integrated with fluorescence imaging using emission discrimination mode. Image (XY) acquisition was done in real-time over variable z-heights.

Live Platelet Imaging: Platelets were pre-incubated (10 mins) with probes as indicated in figures and legends. Fibrillar collagen ($20 \mu\text{g}/\text{mL}$) were used to pre-coat MatTek dishes and then blocked with 2% fatty acid-free BSA. Aliquots of washed platelets suspended in Tyrode's supplemented with 1 mmol/L CaCl_2 were added onto dishes, and platelet activities were monitored in XY or XYZ dimensions over time. High-resolution 3D and 4D images of live-platelets adhering over agonist coated surfaces were obtained at 25°C using a spinning-disk confocal system as described above and previously [4-6].

Image Deconvolution and Analysis: Image resolution was improved by the restoration complement of Volocity 6.3 imaging software (Perkin-Elmer, UK). Point-spread functions specific to the microscope, the refractive index of immersion medium and acquisition lenses numerical aperture was calculated using the action menu of the software, this was then used to conduct iterative restoration of the fluorescent images. Using pre-installed Volocity algorithms, platelet-derived microvesicles were identified by intensity in 3 & 4D data using both Fluo-4 and Annexin-V signal intensities combined with a size discrimination step for vesicles of size between 100nm and $1 \mu\text{m}$, which excluded vesicles $< 100\text{nm}$ and $> 1 \mu\text{m}$ from the analysis output.

Ferric chloride carotid injury model in mouse

Mice were anaesthetised with ketamine 100 mg/kg (Vetalar V, Pfizer) and 10 mg/kg xylazine (Rompun, Bayer). Platelets were labelled by intravenous administration of 100 mg/kg Dylight-488 conjugated anti-GPIIb/IIIa antibody, 10 min prior to induction of thrombosis. Right carotid arteries were exposed and 2x1 mm 12% ferric chloride-soaked filter paper was placed on the arterial adventitia for 3 min. Time-lapse microscopy of the injury site for 20 min was performed and images processed using ImageJ. Background fluorescence values measured upstream of the injury site were subtracted from thrombus-specific fluorescence and data expressed as integrated densities.

Statistical Analysis

Data were analysed using GraphPad Prism 8 (San Diego, CA) and presented as a box with whiskers plots showing min to max values, the medians and interquartile ranges of data. Test for normality was by D'Agostino & Pearson omnibus as well as Shapiro-Wilk tests. We determined statistical significance by the Friedman test, followed by the Dunn multiple comparison tests or by Wilcoxon signed rank test. $P < 0.05$ (*) or $P < 0.01$ (**) was considered significant.

RESULTS

Proteomic and genomic analyses suggest that carbonic anhydrase enzymes 1, 2, and 13 are expressed in human platelets [10-12]. Also, while CA I and II showed tissue-wide expression [13-15], CA XIII showed selective expression in platelets in particular [11, 16]. In this study, we determined the expression of CA I, CA II, and CA XIII in human platelets by western blotting and immunofluorescence (**Fig. 1**).

Changes in platelet volume can be used to measure carbonic anhydrase-dependent chloride/bicarbonate exchange activity [17, 18], and several reports have shown that the bicarbonate-enhanced swelling of platelets and some hematopoietic cells in isotonic solutions of ammonium chloride is abolished by CA inhibitors [17, 18]. We used this approach to confirm platelet CA enzyme activity and their marked inhibition by 100 μ M acetazolamide (ACZ) or methazolamide (MTZ).

Acetazolamide or methazolamide did not consistently alter platelet aggregation or granule secretion in response to Collagen Related peptide or thrombin (**Fig. 2A**). The small inhibition of platelet aggregation observed in washed platelets was not replicated in the more physiological condition of platelet-rich-plasma (PRP) (**Fig. 2A_i**). By contrast, platelet CA enzyme inhibition by ACZ (30, 100 μ M) or MTZ (100 μ M), caused a marked deficit in the formation of procoagulant platelets *in vitro* (**Fig. 2B**); notably, the formation of BNS and BAPS platelets was markedly reduced. Methylation of the amine moiety of the sulfonamide group in acetazolamide, to generate N-methyl-acetazolamide (NMA), ablates its binding to the active site of CA enzymes. NMA, therefore, acts as a negative control inactive analogue, lacking significant inhibition of CA enzyme activity [17, 19]. Pre-treatment of platelets with up to 100 μ M NMA did not affect the formation of procoagulant platelets (**Fig. 2B**); this confirmed that the procoagulation suppression effects of ACZ and MTZ are mediated by inhibition of CA enzyme activity and not by some other action of NMA, such as suppression of hypoxic calcium signaling as demonstrated in pulmonary artery smooth muscle cells [20] Notably, the generation of procoagulant microparticles [4, 5, 8] in human platelets adhering to collagen fibres was diminished after ACZ (**Fig. 2C**) and MTZ (not shown) treatments.

We had previously reported that calcium and chloride influx are pivotal intracellular events mediating the platelet procoagulant response [4, 5]. In medium lacking chloride ions, we showed that membrane ballooning and procoagulant spreading was diminished in collagen-activated platelets [4, 5] as well as in platelets pre-treated with small molecule inhibitors of calcium-activated chloride channels [4]. The inhibitory effect of CA inhibitors on procoagulation is likely mediated through an attenuated chloride entry mechanism, since platelets pre-treated with 100 μ M ACZ showed diminished chloride ion entry after collagen stimulation (**Fig. 3A**). When we examined thrombosis in mice administered methazolamide 10 mg/kg which had been shown to fully inhibit carbonic anhydrase activity [21] the results showed that thrombus formation was markedly diminished (**Fig. 3B**), and was comparable with the previously reported effect of ACZ on *in vivo* thrombosis[4]. Finally, when we used thromboelastometry (ROTEM) in human blood to assess the effect of CA enzyme inhibition on blood clotting parameters. Surprisingly the data showed no significant effects of ACZ or MTZ up 100 μ M on any of the ROTEM parameters examined (**Fig. 4**).

DISCUSSION

The carbonic anhydrases are a family of enzymes that catalyse the rapid interconversion of carbon dioxide and water to bicarbonate and protons ($\text{CO}_2 + \text{H}_2\text{O} \rightleftharpoons \text{HCO}_3^- + \text{H}^+$). Since these enzymes produce and utilize protons and bicarbonate ions, they play a key role in the regulation of pH and fluid balance in mammalian cells. In this study, CA inhibitors ACZ or MTZ did not significantly alter platelet aggregation, alpha or dense granule secretion, or integrin activation in response to collagen and thrombin. This is consistent with our proposed role for CA enzymes as primarily a mediator of the platelet procoagulant response. The secretion sparing action of CA enzymes inhibitors open-up new avenues for the development of novel antithrombotic agents, which will act distinctly from antithrombotics currently used in clinics such as P₂Y₁₂ blockers (clopidogrel, prasugrel, ticagrelor or cangrelor). Recently, we identified water channel, AQP1 as another molecular target that may be modulated to suppress *in vivo* thrombosis while sparing secretion mechanism, effectively acting as antiprocoagulant-antithrombotic[6].

From our work and those of others we know that platelets undergo a dramatic change in shape, ballooning, followed by microvesiculation upon binding to collagen-coated surfaces, to substantially increase the surface area of PS, thereby causing procoagulation[4, 7, 8]. This procoagulant response can be blocked by acetazolamide, which has actions both to block carbonic anhydrase (CA) and water entry channels (including AQPs)[22, 23]. However, ballooning and microvesiculation may be mechanistically distinct because genetic deletion of AQP1 leads specifically to the loss of microvesiculation, and not ballooning[6]. This leaves the question, do carbonic anhydrases have a role to play in addition to AQPs, specifically in regulating ballooning and procoagulation in platelets. This study shows clearly that methazolamide, chemically related to acetazolamide, also has the ability to block the procoagulant and spreading activity of platelets. Methazolamide, in turn, also has marked antithrombotic action in a mouse model of arterial thrombosis. This is clearly tied to the ability of these drugs to block CA, since the inactive analogue, N-methyl acetazolamide, has no effect. This is important since these drugs have actions also to block water channels (including AQPs). Our previous data demonstrate clearly that AQP1 is critical for procoagulant spreading and microvesiculation[6], and the data presented here support the idea that blockade of CA (by acetazolamide and methazolamide) is important for blocking ballooning and procoagulation.

We had previously established that the platelet procoagulant response is preceded by calcium mobilisation from intracellular stores[3, 24]; this is associated with the activation of Ca²⁺ activated chloride channels, which results in an initial salt entry which is then followed by the influx of water[4]. The chloride ion entry causes membrane hyperpolarisation and enhances the electrochemical drive for Ca²⁺ entry[25] through both store-operated and store-independent pathways ensuring the high and sustained level of cytosolic calcium required to drive the procoagulant response[3, 4, 25, 26]. During this process, it is likely that agonist-induced stimulation of a CA-dependent chloride/bicarbonate (Cl⁻/HCO₃⁻) exchanger facilitates the rise in intracellular chloride ion [Cl⁻]_i level at the expense of HCO₃⁻ ions[17-19, 27].

In providing further mechanistic insights into the procoagulant remodelling of the human platelet, our data so far indicate that ion entry through Na⁺ and Cl⁻

channels[4], coupled with water entry through AQP1 [6], is involved in the procoagulant response[4, 5, 8], and therefore that inhibition of either Na⁺, Cl⁻ or water entry (AQP1) can block this response[4, 6-8]. CA inhibitors such as ACZ are also potent direct-acting vasodilators in the cerebral vasculature[28]; with the additional antiprocoagulant antithrombotic activities here reported, specific CA inhibitors may be uniquely effective for the treatment or prevention of cerebral thrombosis or infarction especially in hypertensive patients with heightened Cl⁻/HCO₃⁻ exchanger activity[29]. Taken together, the antiprocoagulant and antithrombotic effects of ACZ and MTZ reported here are likely due to their inhibitory actions on Cl⁻ entry mechanism.

It is likely that the 'no effect' result from our ROTEM analysis is a result of the way ROTEM evaluates haemostatic function. Largely, this is based on the number and responses of platelets in suspension; however, *in vivo*, and in our previous experimental approaches to stimulate platelet ballooning, platelets are adherent to solid matrices. Accordingly, assays monitoring procoagulant dynamics over solid matrixes are likely to reflect ballooning procoagulant activity differently from platelets in suspension, such as in ROTEM, which then may not be very efficient at inducing balloon-dependent procoagulant activity. In addition, we recently showed that once procoagulant, platelets shed adhesion receptors making them less able to aggregate[4]. Thus, the procoagulant potential of these platelets may go undetected by viscoelasticity or impedance-dependent function tests such as TEG™, ROTEM™, Plateletwork™ or VerifyNow™ systems. Our study, therefore, demonstrates the need for a readily usable clinical test for procoagulant activity since outputs from rotational thromboelastometry do not reflect changes in procoagulant activity. Importantly, a recent publication has shown platelet ballooning to occur in response to substantial tissue injury, leading to the identification of ballooned platelets free in suspension in peripheral blood samples [30]. In this case, identification of ballooning was performed by state-of-the-art imaging flow cytometry, which may provide a future diagnostic step, although further modification of the method would be required to allow direct measurement of thrombin generation or procoagulant activity.

In conclusion, carbonic anhydrase (CA) inhibitors open new avenues for the development of novel antithrombotic agents, which act distinctly from antithrombotics currently used in clinics such as P₂Y₁₂ blockers (clopidogrel, prasugrel, ticagrelor or cangrelor). This drug class may be a suitable alternative for specific patient groups, such as in primary prevention of cerebral infarction or stroke in hypertensives with high CA enzyme activity or to reduce bleeding symptoms associated with current use of dual antiplatelet therapy (P₂Y₁₂ + aspirin). Achieving antithrombosis while sparing secretion, as we show in this study, is particularly vital in post-surgery clinical settings such as after stenting or surgical procedures for myocardial infarction, where the actions of platelet releasates supporting tissue healing are desired [31, 32]. CA inhibitors in clinical use could now be evaluated for repurposing as a new class of antithrombotics in translational research, and new CA inhibitors could be developed for the same purpose, as antiprocoagulant antithrombotics. Convincing evidence for the differential role of specific CA isoenzymes in these is now needed and will require the use of specific CA enzyme knockout models (CA I^{-/-}, CA II^{-/-} & CA XIII^{-/-}).

ACKNOWLEDGEMENT

This study was supported by British Heart Foundation (BHF) project grant to AWP and EOA (PG/16/102/32647), a BHF Foundation grant to AWP (PG/15/96/31854) and a Wellcome Trust grant to AWP (RG/15/16/31758). This work was also supported by the Elizabeth Blackwell Institute for Health Research, University of Bristol and the Wellcome Trust Institutional Strategic Support Fund. Lastly, we are grateful for the support of EOA by the Libin Cardiovascular Institute of Alberta, Calgary, Canada.

CONFLICT-OF-INTEREST DISCLOSURE:

The authors declare no competing financial interests or conflict of interest

AUTHORSHIP CONTRIBUTIONS

EOA designed and performed experiments, analyzed data, contributed to the discussion, and wrote and revised the manuscript. CMW, JZ and RA performed experiments. ERS and IH contributed to the discussion and revised the manuscript. AWP designed research and co-wrote and revised the manuscript

REFERENCES

- [1] Fager AM, Wood JP, Bouchard BA, Feng P, Tracy PB. Properties of Procoagulant Platelets-Defining and Characterizing the Subpopulation Binding a Functional Prothrombinase. *Arterioscler Thromb Vasc Biol* 2010;30:2400-2407.
- [2] Heemskerk JWM, Mattheij NJA, Cosemans JMEM. Platelet-based coagulation: different populations, different functions. *Journal of Thrombosis and Haemostasis* 2013;11:2-16.
- [3] Heemskerk JWM, Vuist WMJ, Feijge MAH, Reutelingsperger CPM, Lindhout T. Collagen But Not Fibrinogen Surfaces Induce Bleb Formation, Exposure of Phosphatidylserine, and Procoagulant Activity of Adherent Platelets: Evidence for Regulation by Protein Tyrosine Kinase-Dependent Ca²⁺ Responses. *Blood* 1997;90:2615-2625.
- [4] Agbani EO, Van den Bosch MTJ, Brown E, Williams CM, Mattheij NJA, Cosemans JMEM, Collins PW, Heemskerk JWM, Hers I, Poole AW. Coordinated Membrane Ballooning and Procoagulant Spreading in Human Platelets. *Circulation* 2015;132:1414-1424.
- [5] Agbani EO, Williams CM, Hers I, Poole AW. Membrane Ballooning in Aggregated Platelets is Synchronised and Mediates a Surge in Microvesiculation. *Scientific Reports* 2017;7:1-12.
- [6] Agbani EO, Williams CM, Li Y, van den Bosch MTJ, Moore SF, Mauroux A, Hodgson L, Verkman AS, Hers I, Poole AW. Aquaporin-1 Regulates Platelet Procoagulant Membrane Dynamics and In Vivo Thrombosis *JCI Insight* 2018;3:e99062.
- [7] Agbani EO, Poole AW. Procoagulant Platelets:-Generation, Function and Therapeutic Targeting in Thrombosis. *Blood* 2017;130:2171-2179.
- [8] Agbani EO, Hers I, Poole AW. Temporal contribution of the platelet body and balloon to thrombin generation. *Haematologica* 2017;102:1-3.
- [9] Swenson ER. Safety of carbonic anhydrase inhibitors. *Expert Opinion on Drug Safety* 2014;13:459-472.
- [10] Gilmour KM. Perspectives on carbonic anhydrase. *Comparative Biochemistry and Physiology Part A: Molecular & Integrative Physiology* 2010;157:193-197.
- [11] Kim M-S, Pinto SM, Getnet D, Nirujogi RS, Manda SS, Chaerkady R, Madugundu AK, Kelkar DS, Isserlin R, Jain S, et al. A draft map of the human proteome. *Nature* 2014;509:575-581.
- [12] Siffert W, Gros G. Carbonic anhydrase in human platelets. *The Biochemical journal* 1984;217:727-730. Epub 1984/02/01.
- [13] Campbell AR, Andress DL, Swenson ER. Identification and characterization of human neutrophil carbonic anhydrase. *Journal of Leukocyte Biology* 1994;55:343-348.
- [14] Parkkila S, Rajaniemi H. Carbonic anhydrase activity in peripheral T-lymphocytes and appearance of the activity during their maturation in the thymus. A histochemical demonstration. *Histochemistry* 1989;91:479-482.
- [15] Hudalla H, Michael Z, Christodoulou N, Willis GR, Fernandez-Gonzalez A, Filatava EJ, Dieffenbach P, Fredenburgh LE, Stearman RS, Geraci MW, et al. Carbonic Anhydrase Inhibition Ameliorates Inflammation and Experimental Pulmonary Hypertension. *American Journal of Respiratory Cell and Molecular Biology* 2019 61:512-524.
- [16] Schubert S, Weyrich AS, Rowley JW. A tour through the transcriptional landscape of platelets. *Blood* 2014;124:493-502.
- [17] Maren TH. Carbonic Anhydrase Inhibition. V. N5-Substituted 2 - Acetylamino - 1,3,4 - Thiadiazole - 5 - Sulfonamides: Metabolic Conversion and Use As Control Substances. *Journal of Pharmacology and Experimental Therapeutics* 1956;117:385-401.
- [18] Vaitkevicius H, Turner I, Spalding A, Lockette W. Chloride increases adrenergic receptor-mediated platelet and vascular responses. *American journal of hypertension* 2002;15:492-498. Epub 2002/06/21.
- [19] Relman AS, Porter R, Tobias JF, Schwartz WB. The diuretic effects of large doses of acetazolamide and an analog lacking carbonic anhydrase inhibiting activity. *The Journal of clinical investigation* 1960;39:1551-1559.

- [20] Shimoda LA, Luke T, Sylvester JT, Shih H-W, Jain A, Swenson ER. Inhibition of hypoxia-induced calcium responses in pulmonary arterial smooth muscle by acetazolamide is independent of carbonic anhydrase inhibition. *American Journal of Physiology-Lung Cellular and Molecular Physiology* 2007;292:L1002-L1012.
- [21] Fanous MM, Challa P, Maren TH. Comparison of Intraocular Pressure Lowering by Topical and Systemic Carbonic Anhydrase Inhibitors in the Rabbit. *Journal of Ocular Pharmacology and Therapeutics* 1999;15:51-57.
- [22] Gao J, Wang X, Chang Y, Zhang J, Song Q, Yu H, Li X. Acetazolamide inhibits osmotic water permeability by interaction with aquaporin-1. *Analytical biochemistry* 2006;350:165-170.
- [23] Zhang J, An Y, Gao J, Han J, Pan X, Pan Y, Tie L, Li X. Aquaporin-1 Translocation and Degradation Mediates the Water Transportation Mechanism of Acetazolamide. *PLOS ONE* 2012;7:e45976.
- [24] Varga-Szabo D, Braun A, Nieswandt B. STIM and Orai in platelet function. *Cell Calcium* 2011;50:270-278.
- [25] Harper MT, Poole AW. Chloride channels are necessary for full platelet phosphatidylserine exposure and procoagulant activity. *Cell Death Dis* 2013;4:e969.
- [26] Varga-Szabo D, Braun A, Nieswandt B. Calcium signaling in platelets. *Journal of Thrombosis and Haemostasis* 2009;7:1057-1066.
- [27] Spalding A, Vaitkevicius H, Dill S, MacKenzie S, Schmaier A, Lockette W. Mechanism of Epinephrine-Induced Platelet Aggregation. *Hypertension* 1998;31:603-607.
- [28] Berthezene Y, Nighoghossian N, Meyer R, Damien J, Cinotti L, Adeleine P, Trouillas P, Froment JC. Can cerebrovascular reactivity be assessed by dynamic susceptibility contrast-enhanced MRI? *Neuroradiology* 1998;40:1-5.
- [29] Alonso A, Arrázola A, Garciandía A, Esparza N, Gómez-Alamillo C, Díez J. Erythrocyte anion exchanger activity and intracellular pH in essential hypertension. *Hypertension* 1993;22:348-356.
- [30] Vulliamy P, Gillespie S, Armstrong PC, Allan HE, Warner TD, Brohi K. Histone H4 induces platelet ballooning and microparticle release during trauma hemorrhage. *Proceedings of the National Academy of Sciences* 2019:201904978.
- [31] Walsh TG, Poole AW. Do platelets promote cardiac recovery after myocardial infarction: roles beyond occlusive ischemic damage. *Am J Physiol Heart Circ Physiol* 2018;314:H1043-H1048. Epub 2018/03/16.
- [32] Walsh TG, Poole AW. Platelets Protect Cardiomyocytes from Ischemic Damage. *TH Open* 2017;01:e24-e32.

Figures And Legends

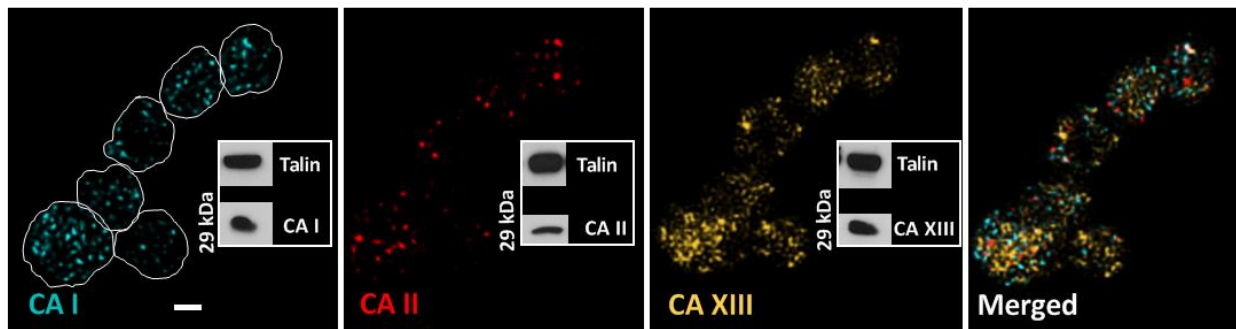


Figure 1: Spatial Distribution of Carbonic Anhydrase I, II & XIII in Human Platelets. Human platelets applied to bovine serum-coated surfaces were probed for the expression of carbonic anhydrase (CA) enzymes I, II and XIII by immunocytochemistry. Left hand panel describes outline of each platelet by a thin white line. Inset shows the respective immunoblot for CA enzymes I, II and XII from human platelet lysates, together with talin as a loading control. Scale bar represents 3 μ m. Data are from 4 independent experiments.

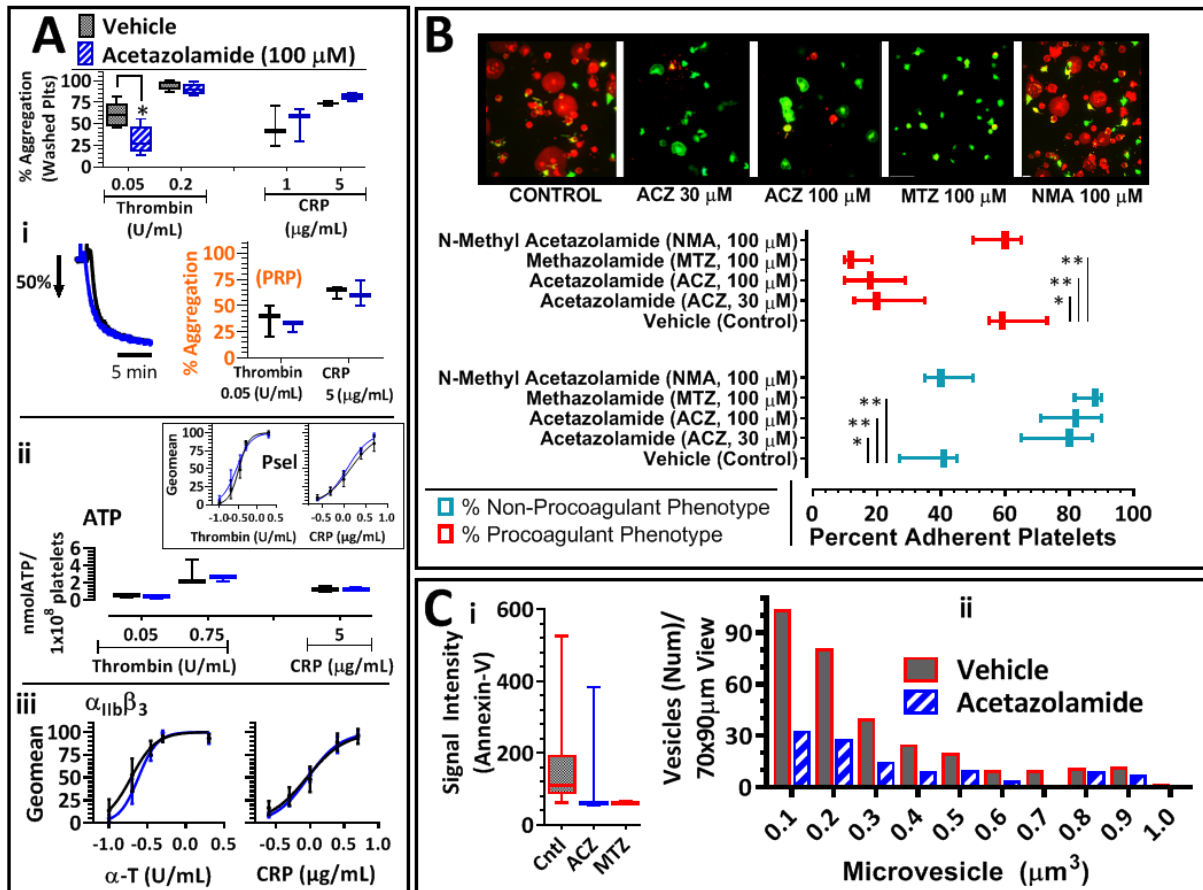


Figure 2: Acetazolamide and Methazolamide Suppressed the Platelet Procoagulant Response but not Aggregation or Secretion. In **A-i**, human platelets (washed or in plasma) were stimulated with thrombin or collagen-related peptide (CRP) and percent aggregation was assessed by optical aggregometry. The figures show example aggregation traces and interleaved box plots with whiskers indicating minimum to maximum values, median, and interquartile range of percent aggregation (N = 4). In **A-ii**, platelets were stimulated for 10 min with a range of concentrations of thrombin or CRP in the presence of 1 mM CaCl₂. Top graphs show P-selectin exposure (Psel) profile as determined by flow cytometry. Lower chart is the interleaved box plots of ATP release data as measured by luminometry. The plot whiskers show minimum to maximum values, median, and interquartile range of ATP secretion (N=4). In **A-iii**, integrin $\alpha_{IIb}\beta_3$ activation was determined by flow cytometry using PAC-1 antibody. For flow cytometry data in **A-ii** and **A-iii**, the geometric mean of the fluorescence intensity was determined, and data are shown as the percentage of maximal control response (N = 4). Curves were fitted by F-test. **B**: Acetazolamide and methazolamide, but not N-methyl acetazolamide, attenuate the human platelet procoagulant response to collagen. Platelets were preincubated with DMSO (Vehicle, Control), acetazolamide (ACZ, 100 μ M), methazolamide (MTZ, 100 μ M), or N-methyl acetazolamide (NMA, 100 μ M) and allowed to adhere to fibrillar collagen and then imaged after 1hr. Charts show percent variation in the formation of platelet phenotypes previously identified as non-procoagulant (CSNB: conventional-spread non-ballooned platelet; NBNS: non-ballooned non-spread platelets) or procoagulant (BNS: ballooned non-spread platelets; BAPS: ballooned and procoagulant-spread platelet). Images are annexin-V (Red) superimposed with corresponding Fluo-4 images (Green) and were obtained by spinning-disk confocal microscopy at x 100 objective magnification (N = 4). **C**: Charts (**C-i**) show signal intensity of annexin-V binding on platelet membranes and (**C-ii**) the size distribution of microvesicles formed over collagen-coated surface. The chart in **B** and **C-i** is interleaved box plots with whiskers showing minimum to maximum values, median, and interquartile ranges. Microvesiculation was determined by image-based particle counting method. Microvesicles were AnnexinV + and between 100 nm and 1 μ m diameter. Scale

bars represent 5 μm (B). * and ** indicate $p < 0.05$ and $p < 0.01$, respectively. Data are from 4 independent experiments.

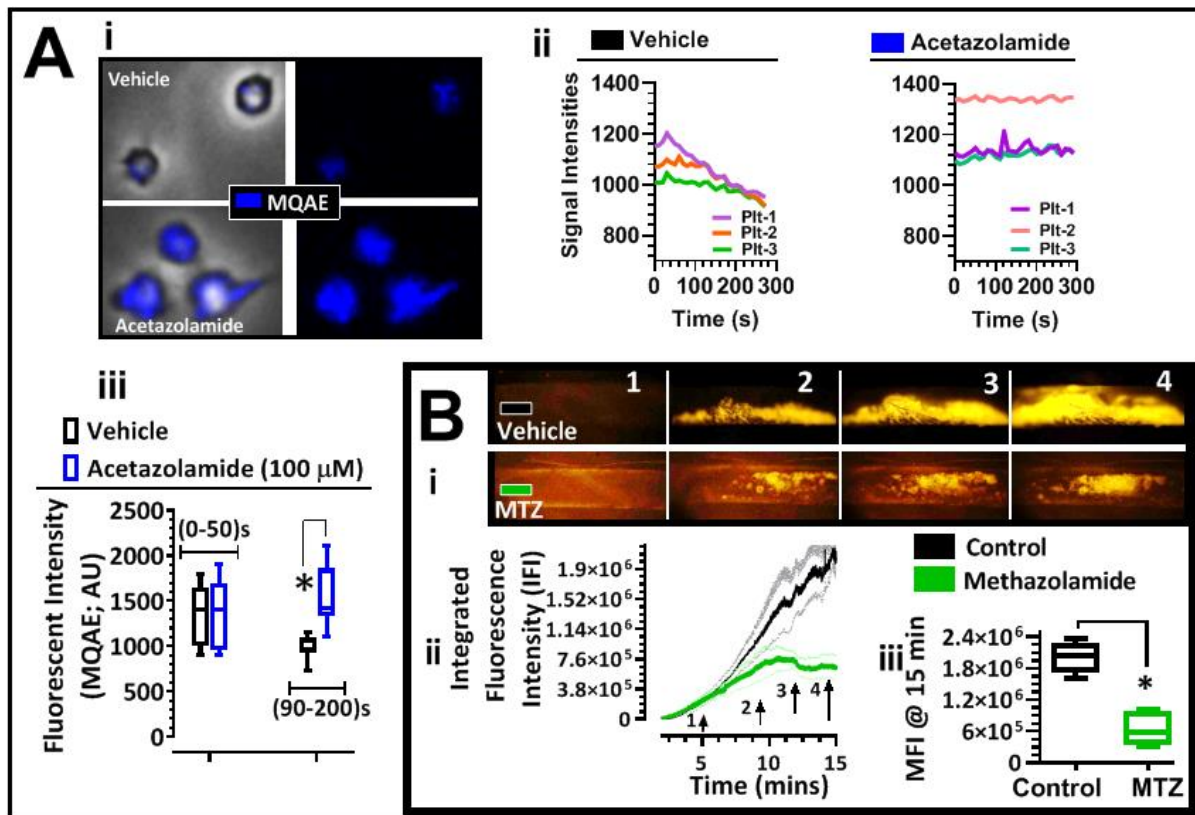


Figure 3: Carbonic Anhydrase Inhibitors Suppress In Vitro Collagen-Induced Chloride Ion Entry and In Vivo Thrombosis. **A-i**, show images of platelets adherent onto immobilised collagen. Platelets had been preloaded with the chloride ion (Cl^-) indicator, N-(Ethoxycarbonylmethyl)-6-methoxyquinolinium bromide (MQAE) and preincubated with DMSO (top row) or acetazolamide 100 μM (bottom row). Images are MQAE alone (blue) or overlaid onto phase-contrast images and show early phases of remodelling after activation. MQAE detects chloride ion entry by collisional quenching, therefore decreases in signal intensity (F/F_0) for MQAE observed in **A-ii**, (vehicle) represent increases in intracellular chloride ion concentration. **A-ii** show plots of MQAE vs time in representative platelets. **A-iii** show plot of MQAE signal for over 140 platelets at time points shown. **B**: C57-Bl6 mice were administered methazolamide 10 mg/kg to suppress carbonic anhydrase enzyme activity and DyLight 488–conjugated anti-GPIIb β antibody to label platelets. The carotid artery was damaged using FeCl_3 and fluorescently labelled platelets were imaged by intravital microscopy. Image number indicated in **B-i** corresponds to time points indicated in **B-ii**, which shows the time course of change in fluorescence intensity for thrombus formation. In **B-iii**, median thrombus fluorescence intensity (MFI) at 15 min is shown as interleaved box plots with whiskers showing minimum to maximum values, median and interquartile range. Scale bar in **A** and **B** represents 5 and 500 μm , respectively. * indicate $p < 0.05$. Data are from 6 independent experiments.

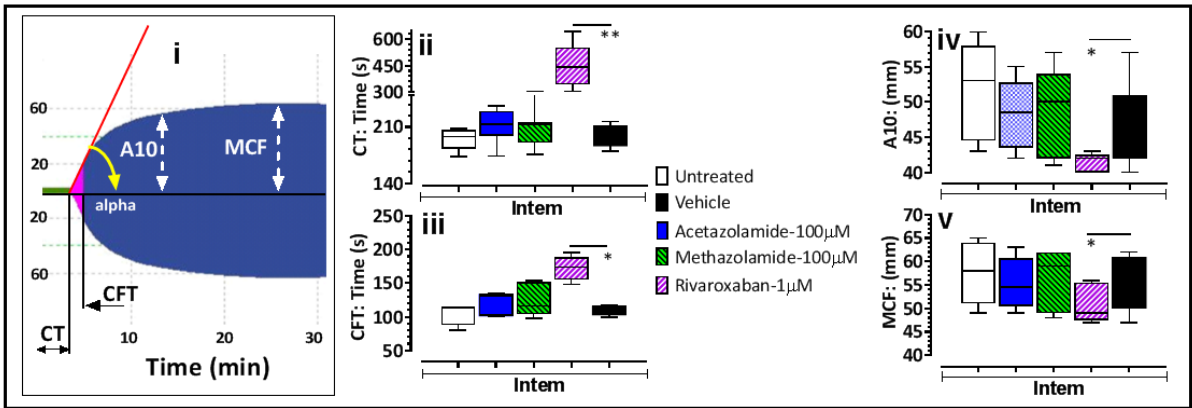


Figure 4: Rotational Thromboelastometry (ROTEM) Assessment of Healthy Human Donor Blood Treated In Vitro with Carbonic Anhydrase Inhibitors. The figure shows clotting time (CT) and clot formation time (CFT) for human blood samples treated with acetazolamide, methazolamide, vehicle or rivaroxaban. In (i), a graphical representation of ROTEM analysis is shown. Clotting time CT (seconds) represents the beginning of the test until a clot firmness of 2 mm while CFT (seconds) represents time to achieve a clot firmness of 20 mm. The alpha angle is the angle of tangent between 0 mm and the curve when the clot firmness is 20 mm. A10 values describe the clot firmness (or amplitude) obtained after 10 minutes from CFT. Maximum clot firmness MCF is the greatest vertical amplitude of the trace. Sub-panels ii-v show the mean of these parameters plotted as interleaved box plots with whiskers showing minimum to maximum values and interquartile range. Data are from 8 human donors.